

Published in final edited form as:

Kidney Int. 2011 March ; 79(5): 538–545. doi:10.1038/ki.2010.458.

1,2,3,4,6-penta-O-galloyl-beta-D-glucose (PGG) reduces renal crystallization and oxidative stress in a hyperoxaluric rat model

Hyo-Jung Lee^{a,#}, Soo-Jin Jeong^{a,#}, Hyo-Jeong Lee^a, John C. Lieske^{b,*}, and Sung-Hoon Kim^{a,b,*}

^aCollege of Oriental Medicine, Kyunghee University, Seoul 130-701, Republic of Korea

^bDepartment of Internal Medicine, Division of Nephrology and Hypertension, Mayo Clinic College of Medicine,, Rochester, Minnesota 55905, USA

Abstract

Adhesion of calcium oxalate (CaOx) crystals to kidney cells may be a key event in the pathogenesis of kidney stones associated with marked hyperoxaluria. Previously, we found that 1,2,3,4,6-penta-O-galloyl-beta-D-glucose (PGG), isolated from a traditional medicinal herb, reduced CaOx crystal adhesion to renal epithelial cells by acting on the cells as well as the crystal surface. Here we used the ethylene glycol (EG) - mediated hyperoxaluric rat model and found evidence of oxidant stress as indicated by decreases in the activities of the renal antioxidant enzymes superoxide dismutase, catalase, and glutathione peroxidase, with increased kidney cell apoptosis and serum malondialdehyde levels, all evident by 21 days of EG treatment. These effects of hyperoxaluria were reversed by concurrent PGG treatment along with decreased urinary oxalate levels and CaOx supersaturation. Renal epithelial cell expression of the crystal binding molecule hyaluronan increased diffusely within 7 days of EG initiation, suggesting it is not a result of but precedes crystal deposition. Renal cell osteopontin (OPN) was also up regulated in EG-treated animals, and PGG significantly attenuated over expression of both OPN and hyaluronan. Thus, our findings demonstrate that PGG reduces renal crystallization and oxidative renal cell injury, and may be a candidate chemo preventative agent for nephrolithiasis.

INTRODUCTION

The majority (~70%) of human kidney stones contain calcium oxalate (CaOx). However, the mechanisms of renal stone formation are poorly understood. Although urinary supersaturation with calcium and oxalate is known important factor, the treatment strategies aimed to reduce urinary supersaturation are only partially effective, stone recurrence is still common and stone recurrence is still common. Furthermore, the pathways from urinary supersaturation to kidney stone are poorly defined. In states of marked hyperoxaluria, such

*Corresponding authors: **Sung-Hoon Kim**, College of Oriental Medicine, Kyunghee University, 1 Hoegi-dong, Dongdaemun-gu, Seoul 131-701, Republic of Korea. sungkim7@khu.ac.kr, **John C. Lieske**, Department of Internal Medicine, Division of Nephrology and Hypertension, Mayo Clinic College of Medicine,, 200 First Street SW, Rochester, Minnesota 55905, USA. Lieske.john@mayo.edu (J.C.Lieske).

#These authors contributed equally to this work.

DISCLOSURE

All the authors declared no competing interests.

as primary and enteric hyperoxaluria, oxalate-induced oxidative stress and/or adhesion of CaOx crystals to renal cells may be important events. In all types of stone disease additional therapeutics are required¹.

Several recent studies have highlighted the effectiveness of several Oriental medicinal herbs or natural compounds for the treatment of nephrolithiasis. For example, Al-Ghamdi and colleagues demonstrated that *Cymbopogon schoenanthus* extract inhibited calcium oxalate deposition in ethylene glycol-treated male Wistar albino rats². Similarly, Yuliana and colleagues demonstrated that methoxy flavonoids from *Orthosiphon stamineus* Benth, an Indonesian medicinal herb, can prevent crystallization in a rat kidney stone model³. Green tea and its major component, epigallocatechin-3-gallate were also reported to inhibit kidney stone formation *in vitro* and *in vivo*^{4,5}. Recently, our group reported that 1,2,3,4,6-penta-O-galloyl-beta-D-glucose (PGG), a water soluble gallotannin just like epigallocatechin-3-gallate, attenuates calcium oxalate crystal adhesion to renal epithelial cells, perhaps via effects on hyaluronan expression⁶.

Therefore, the current study was conducted to evaluate the *in vivo* efficacy of PGG for the prevention of crystallization, renal injury, and oxidative stress in a hyperoxaluric rat model induced by 0.8% EG and 1% ammonium chloride.

RESULTS

PGG reduces crystalluria and urinary oxalate excretion in EG-treated rats

Rats were studied 7, 14, and 21 days after initiation of EG treatment. PGG significantly reduced CaOx crystalluria (Figure 1a), intrarenal CaOx crystal deposition (Figure 1b), and urinary oxalate excretion (Table 1) compared with animals treated with EG alone. Renal function was preserved in all animals for this 3-week study (Table 2). Urinary oxalate excretion and CaOx supersaturation, assessed using the AP Tiselius index,⁷ were both decreased by PGG at the higher 20 mg/kg dose (Table 1).

Oxalate increases ROS production and induces oxidative renal cell injury in human renal cells

Previous studies have suggested that oxalate can injure renal cells, in part, through oxidative stress pathways,⁸ and this injury may promote renal crystal deposition.⁹ To assess the effect of PGG on oxalate-induced oxidative stress, human renal cells (HRCs) were exposed to 1mM oxalate *in vitro*. PGG at 25 or 50 mM markedly reduced reactive oxygen species (ROS) production of the cells from 33 to 8.3% and 5%, respectively (Figure 2a). Serum malondialdehyde (MDA) levels were also increased by day 21 in EG-treated animals, and this increase was blunted by concurrent administration of PGG (Figure 2b).

PGG enhances antioxidant enzyme activities in hyperoxaluric rat kidneys

To further define the effects of PGG on oxalate-induced oxidative stress, intrarenal expression of antioxidant enzymes was analyzed. EG treatment reduced renal superoxide dismutase (SOD) expression at 7 and 14 days, and even more dramatically by day 21 (Figure 3a). Concurrent administration of PGG, however, increased renal SOD by

immunohistochemistry (Figure 3a) or western blot (Figure 3b). Similarly, PGG significantly enhanced renal expression of the antioxidant enzymes catalase and glutathione peroxidase in EG-treated rats (Figure 3c).

PGG significantly reduces renal osteopontin expression and apoptosis induced by hyperoxaluria

Previous studies have suggested that renal expression of OPN is upregulated in response to renal injury, 10–12 including that induced by EG.¹³ Immunohistochemistry and western blotting confirmed that renal expression of OPN was enhanced 21 days after initiation of EG treatment (Figure 4). PGG significantly blunted this increase in OPN expression in a dose-dependent manner (Figure 4). To further evaluate a potential protective effect of PGG, renal cell apoptosis was assessed by terminal deoxytransferase uridine triphosphate nick end labeling (TUNEL) assay. The number of TUNEL-positive cells was dramatically increased by EG treatment to 24%, but this increase was dramatically blunted by concurrent PGG treatment (9 and 7% at 4 and 20 mg/kg, respectively, (Figure 5). These results suggest that PGG can prevent oxalate-induced renal cell injury induced by EG.

PGG attenuates renal hyaluronan expression in EG-treated rat kidneys

Hyaluronan (hyaluronic acid) is secreted and expressed by proliferating renal tubular cells as a crystal-binding molecule.^{14–17} In our previous study, PGG decreased hyaluronan expression in scrape-wounded MDCK I cell monolayers.⁶ In the current in vivo study, PGG also significantly reduced renal tubular cell hyaluronan expression on days 7 and 14 after initiation of injury by hyperoxaluria (Figure 6). Furthermore, the increase in hyaluronan expression was diffuse and did not colocalize with crystal deposits (Figure 6a).

DISCUSSION

Nephrolithiasis is a common, painful, and costly condition. CaOx stones are by far the most common, accounting for up to 70% of cases.¹⁸ Among those with extreme hyperoxaluria, such as seen in patients with primary or enteric hyperoxaluria, oxalate-induced cell damage and crystal adhesion to cells have been implicated. Hyperoxaluric rat models are often used to model these events, either induced by EG alone^{19,20} or in combination with ammonium chloride.^{18,21} Therefore, in this study, the mechanism(s) whereby PGG isolated from a gallnut of *Rhus chinensis* MILL or *Paeonia lactiflora* alters CaOx crystal adhesion to cells and oxalate induced renal cell injury was examined in rats treated with 0.8% EG and 1% ammonium chloride for 1, 2, and 3 weeks to confirm our previous in vitro data that PGG inhibits kidney stone formation.⁶

Kidney stone formation involves a cascade of events including one or more of the following: urinary supersaturation, crystal nucleation, growth, and aggregation; retention of crystals in the renal tubules or interstitium; and growth of a calculus upon a tubular plug or interstitial deposit (so-called Randall's Plaque).²² In this study, PGG significantly decreased renal CaOx crystal deposition compared with animals treated with EG alone. Our results suggest that multiple factors may contribute to the protective effect of PGG, including decreased urinary oxalate excretion and supersaturation, decreased renal oxidative injury, and

decreased expression of the renal cell crystal binding molecule hyaluronan. Our previous *in vitro* study also suggested that PGG can exert effects on the surface of CaOx crystals and renal cells that decrease their propensity to adhere.⁶

Evidence implicates free radical production, lipid peroxidation, and renal tubular epithelial cell injury during kidney stone formation.^{9,23,24} Therefore, antioxidant agents such as epigallocatechin-3-gallate, vitamin E, DL α '-lipoic acid, and green tea were considered potential therapeutics for kidney stone formation.^{5,22,25,26} Atorvastatin, a cholesterol-lowering drug with antioxidant activity, was also reported to inhibit renal crystal retention in a rat stone-forming model.²⁷ Nonetheless, the relationship between CaOx crystal deposition and oxidative stress remains unclear. Thamilselvan et al.²⁹ suggested that oxalate-associated free radical injury can promote stone formation,²⁸ in part, due to hyperoxaluria-induced peroxidative injury and enhanced CaOx crystal attachment to renal tubules. Similarly, Schepers et al.³⁰ demonstrated that CaOx crystals generate ROS and cause acute inflammation-mediated necrotic cell death of renal proximal tubular cells. Not all studies support this proposed pathway, as Green et al.³¹ did not find evidence of lipid peroxidation in their hyperoxaluric rat model.

Previous *in vitro* studies suggested that renal cells exposed to oxalate and/or CaOx crystals generate ROS, thereby inducing injury and inflammation.^{32,33} Our *in vitro* studies confirmed that 1mM oxalate increased ROS generation in cultured HRCs, and that this effect was blunted by PGG. PGG also prevented an increase in serum MDA levels among EG-treated animals, increased renal levels of antioxidants, and reduced the number of TUNEL-positive cells. Although the specificity of the TUNEL assay for apoptosis versus necrosis has been questioned,³⁴ these results all suggest that PGG can protect against the ROS-induced renal cell injury death that is associated with EG-induced hyperoxaluria. Interestingly, however, PGG also reduced urinary oxalate excretion and urinary CaOx supersaturation in the EG treated animals. The mechanism(s) of this effect is currently unknown. However, we cannot rule out the possibility that the reduction in urinary oxalate levels, in part, mediated the positive effect of PGG in this model. It is important to point out, however, that renal antioxidant levels were increased (rather than unchanged) in EG animals given PGG (Figure 3), and that PGG prevented ROS generation by oxalate-treated HRCs *in vitro* (Figure 2). Furthermore, renal hyaluronan expression was increased within 7 days exposure to EG, and hyaluronan overexpression was blunted by concurrent PGG administration.

Interestingly, the hyaluronan staining was diffuse and not restricted to areas of crystal deposition, suggesting that hyaluronan may be overexpressed by multifactors including renal cell injury or crystallization. Our previous *in vitro* studies using cultured cells also suggested that PGG reduced hyaluronan expression on the surface of proliferating cells.⁶ Furthermore, PGG decreased OPN overexpression associated with renal injury induced by EG, suggesting potential anti-inflammatory effects. Therefore, our evidence suggests that PGG reduces urinary retention of CaOx crystals in hyperoxaluric rats, perhaps due to decreased renal injury and resulting expression of crystal binding molecules.

In summary, PGG significantly reduced urinary oxalate excretion, CaOx supersaturation, and renal CaOx crystal deposition in rats rendered hyperoxaluric with EG. Furthermore, when given together with EG, PGG reduced a serum marker of oxidative stress (MDA), enhanced the renal activities of antioxidant enzymes (SOD, catalase, and glutathione peroxidase), downregulated renal expression of crystal binding molecules (hyaluronan and OPN), and reduced renal signs of injury (number of TUNEL-positive cells). PGG also reduced oxalate-induced ROS generation by cultured HRCs in vitro. Taken together, our findings demonstrate that PGG reduces renal crystallization and oxidative renal cell injury by its antioxidant and anti-CaOx crystal binding activities, and is a candidate chemopreventive agent for nephrolithiasis.

MATERIALS AND METHODS

Isolation and identification of PGG

Gallnut of *R. chinensis* MILL was obtained from the Oriental Medical Hospital of Kyung Hee University in Seoul and kindly authenticated by professor Namin Baek in the Department of Oriental Herbal Materials, Kyung Hee University. The methanol extract (252 g) was dissolved in distilled water (800 ml) and successively fractionated with equal volumes of n-hexane, ethyl acetate, and butanol with water; the resulting butanol fraction (35 g) was subjected to silica gel column chromatography and eluted by chloroform, methanol and H₂O (65:35:10) and ethyl acetate, methanol and H₂O (100:15.6:13.5), followed by purification using high-performance liquid chromatography (J'sphere ODS-HP80, Kyoto, Japan, 250_20mm ID, S-4 mm, 80A, ethyl acetate/methanol/H₂O^{1/4}6:3:1). The active compound was identified as PGG (molecular weight^{1/4}4940) by nuclear magnetic resonance and fast atom bombardment mass spectrometry analysis with a purity of 498% (ref. 35).

Animals

Sprague–Dawley rats weighing 200–220 g (male; n^{1/4}24) were purchased from Nara Biotech (Seoul, Republic of Korea) and given food and water ad libitum. Rats were housed in a room maintained at 25±1 °C with 55% relative humidity.

Kidney stone model and PGG administration

The rats were divided into four groups (six rats/group): Control group, EG-treated group, EG+PGG 4 mg/kg group, and EG+PGG 20 mg/kg group. Control group rats were given distilled water, whereas EG-treated animals had 0.8% EG/1% ammonium chloride (NH₄Cl) added to their drinking water to induce hyperoxaluria. EG+PGG animals were given 0.8% EG/1% ammonium chloride (NH₄Cl) dissolved in their drinking water plus 4 or 20 mg/kg PGG dissolved in 2% methylcellulose by gastric lavage daily for 21 days. On days 7, 14, and 21 from the beginning of EG treatment, 24-h urine samples were collected on ice in metabolic cages to measure the excretion of oxalate and calcium, and blood samples were collected from the inferior vena cava of rats under ether anesthesia and immediately frozen at -80 °C before using. The right kidneys were stored at -70 °C after quick freezing under liquid nitrogen and the left kidney was fixed in 4% paraformaldehyde for physiological examination.

Renal histology

Paraffin-embedded sections (4 mm) of rat kidneys were stained with hematoxylin and eosin (H&E) to quantify crystallization. The number of crystal deposits in kidney tissue was counted in 10 randomly selected fields and photographed under an Axiovert S 100 light microscope (Carl Zeiss, Weimar, Germany) at $\times 400$ magnification.

Urinalysis

Twenty-four hour rat urine samples on days 7, 14, and 21 were collected on ice in a metabolic cage, and sodium azide was used as a preservative in the sample collecting tubes containing 6N HCl to prevent the non-enzymatic conversion of ascorbate to oxalate during urine collection. The urine was centrifuged at 1300 g for 15 min, the pellets were resuspended in 50 ml of water, and crystal size and quantity were observed in a hemocytometer at $\times 400$ magnification under an Axiovert S 100 light microscope (Carl Zeiss). To measure oxalate concentration in rat urine, reaction reagents were prepared as follows: reagent A (50mM succinate buffer containing 0.79mM dimethylaniline and 0.11mM 3-methyl-2-benzothiazolinone hydrazone, reagent B (100mM EDTA), reagent C (200mM oxalic acid solution, pH 3.8, 37 °C), and reagent D (peroxidase enzyme solution). All reagents were equilibrated to 37 °C before using and mixed with rat urine or standards (oxalic acid) by inversion. Then, reagent E (oxalate oxidase, 0.5 U/ml) was immediately added to the mixture and incubated for 2 h at room temperature in dark. Optical density was measured using microplate reader (Molecular Devices, Sunnyvale, CA) at 600 nm.

Concentrations of urine calcium, magnesium, and citrate were measured by the Green Cross Reference Laboratory (Yonling, Republic of Korea) using Hitachi 747 automatic analyzer (Hitachi, Tokyo, Japan) by ion selective electrode method. The ion activity product of CaOx (AP (CaOx)) was calculated based on the urinary values of oxalate, calcium, magnesium, citrate, and volume, according to the following formula: $[(4067 \times \text{Ca}^{0.93} \times \text{Ox}^{0.96}) \times (\text{Mg}^{-0.55} \times (\text{Cit} + 0.015)^{-0.60} \times V^{-0.99})]$, derived from AP (CaOx) Tiselius index,³⁶ originally used for human urine.⁷

Immunohistochemistry

Kidney specimens were immediately removed from killed rats and immunohistochemistry was performed. Kidney tissues were fixed in 10% neutral-buffered formalin overnight, embedded in paraffin, and sectioned (4 mm thickness). Kidney sections were immobilized and deparaffinized by immersion in xylene, dehydrated in a graded series of ethanol and washed with distilled water. For antigen retrieval, the kidney sections were boiled in 10mM sodium citrate buffer (pH 6.0) for 10 min and cooled at room temperature. After washing with tris-buffered saline (TBS), endogenous peroxidase activity was blocked by incubation in 3% H₂O₂-methanol for 10 min at room temperature. The sections were stained with anti-hyaluronic acid binding protein (Seikagaku, Tokyo, Japan), SOD (Assay Designs, Ann Arbor, MI), and OPN (Santa Cruz Biotechnologies, Santa Cruz, CA) overnight at 4 °C using avidin-biotin complex and diaminobenzidine kits (Vector Lab, Burlingame, CA) and also counterstained with Mayer's hematoxylin solution (Sigma chemical, St Louis, MO).

TUNEL staining was performed using a TdT-FragEL DNA fragmentation kit (Oncogene, Boston, MA) and counterstained with methyl green. All stained sections were photographed under an Axiovert S 100 light microscope (Carl Zeiss) at 400 magnification.

MDA assay

MDA content in serum was measured using Bioxytech MDA-586 Assay kit (OXIS International, Portland, OR).

Cell culture

Human primary renal epithelial cells (HRCs) were isolated from the urine of a healthy, non-stone-forming male using the method of Dorrenhaus et al.,³⁷ as previously described.³⁸ Cells were maintained in Dulbecco's modified Eagle's medium (Welgene, Deagu, Republic of Korea) supplemented with fetal bovine serum and 100 U/ml penicillin and 100 mg/ml streptomycin at 37°C in a humidified atmosphere containing 5% CO₂.

Measurement of ROS generation

2,7-Dichlorofluorescein diacetate was used to measure the levels of ROS induced by oxalate in cultured cells. HRCs (2 × 10⁵ cells) were exposed to oxalate (1mM) for 1 h, and then to 20 mM 2,7-dichlorofluorescein diacetate. After 30 min incubation at 37°C, fluorescence intensities were measured by flow cytometry (BD FACSCalibur, Becton Dickinson, Franklin Lakes, NJ).

Western blot analysis

Homogenized kidney tissues were lysed in 500 µl of lysis buffer (50mM Tris-HCl, pH 7.4, 150mM NaCl, 1% Triton X-100, 0.1% SDS, 1mM EDTA, 1mM Na₃VO₄, 1mM NaF, protease inhibitor cocktail) for 20min on ice. Lysates were centrifuged at 14,000g for 20min at 4 °C and the protein content of the supernatant was measured using a Bio-Rad DC protein assay kit II (Bio-Rad, Hercules, CA). The lysates containing 20mg of protein were mixed with 4× NuPAGE LDS sample buffer and boiled for 5min. The proteins were separated on 4–12% NuPAGE Bis-Tris gels (Invitrogen, Carlsbad, CA) with 1× NuPAGE MES SDS running buffer and then electrotransferred onto a Hybond enhanced chemiluminescence transfer membrane with transfer buffer (25mM Tris, 250mM glycine, 20% methanol) at 300mA for 90min. The membranes were blocked with 5% nonfat dry milk in TBS buffer containing 0.1% Tween-20 (TBST) for 90min at room temperature, then immunoblotted with primary antibodies of rabbit polyclonal to catalase (1:1000) (Ab Frontier, Yongin, Republic of Korea), SOD (1:1000) (Assay Designs), glutathione peroxidase (1:1000) (Ab Frontier), mouse polyclonal to osteopontin (OPN) (1:1000) (Santa Cruz Biotechnologies) in TBST that contained 5% nonfat dry milk in overnight at 4 °C. After three successive washing with TBST for 10min, the membranes were incubated with goat anti-mouse immunoglobulin-G horseradish peroxidase-conjugated secondary antibody (1:3000 dilution) or goat anti-rabbit immunoglobulin-G horseradish peroxidase-conjugated secondary antibody (1:3000 dilution) in TBST that contained 3% nonfat dry milk for 90 min at room temperature. After three successive washing with TBST for 10min, the proteins were developed using an enhanced chemiluminescence Western blotting detection kit and

exposed to X-ray films. Protein contents were normalized by probing the same membrane with anti- β -actin antibody (Sigma). For β -actin detection, previously used membranes were soaked in stripping buffer (62.5mM Tris-HCl, pH 6.8, 150mM NaCl, 2% SDS, 100mM β -mercaptoethanol) at 65 °C for 30min and hybridized with anti- β -actin (1:20,000 dilution).

Statistical analyses

All data were expressed as means \pm s.d. The statistically significant differences were calculated by Student's t-test for *in vitro* assay and one- or two-way analysis of variance by Duncan's test for *in vivo* assays. P-value ≤ 0.05 was considered as statistically significant.

Supplementary Material

Refer to Web version on PubMed Central for supplementary material.

Acknowledgments

This work was partially supported by a Korea Science and Engineering Foundation (KOSEF) grant funded by the Korean government (MEST) (no. 2009-0063466) to Sung-Hoon Kim, and by grants from the O'Brien Urology Research Center at the Mayo Clinic (National Institutes of Health P50 DK083007) and the Rare Kidney Stone Consortium (National Institutes of Health U54 DK083908) to John C Lieske.

References

1. Saita A, Bonaccorsi A, Motta M. Stone composition: where do we stand? *Urol Int.* 2007; 79(Suppl 1):16–19. [PubMed: 17726347]
2. Al-Ghamdi SS, Al-Ghamdi AA, Shammah AA. Inhibition of calcium oxalate nephrotoxicity with *Cymbopogon schoenanthus* (Al-Ethkher). *Drug Metab Lett.* 2007; 1:241–244. [PubMed: 19356049]
3. Yuliana ND, Khatib A, Link-Struensee AM, Ijzerman AP, et al. Adenosine A1 receptor binding activity of methoxy flavonoids from *Orthosiphon stamineus*. *Planta Med.* 2009; 75:132–136. [PubMed: 19137497]
4. Itoh Y, Yasui T, Okada A, Tozawa K, et al. Preventive effects of green tea on renal stone formation and the role of oxidative stress in nephrolithiasis. *J Urol.* 2005; 173:271–275. [PubMed: 15592095]
5. Jeong BC, Kim BS, Kim JI, Kim HH. Effects of green tea on urinary stone formation: an *in vivo* and *in vitro* study. *J Endourol.* 2006; 20:356–361. [PubMed: 16724910]
6. Lee JH, Yehl M, Ahn KS, Kim SH, et al. 1,2,3,4,6-penta-O-galloyl-beta-D-glucose attenuates renal cell migration, hyaluronan expression, and crystal adhesion. *Eur J Pharmacol.* 2009; 606:32–37. [PubMed: 19374853]
7. Tiselius HG. Aspects on estimation of the risk of calcium oxalate crystallization in urine. *Urol Int.* 1991; 47:255–259. [PubMed: 1781112]
8. Tungsanga K, Sriboonlue P, Futrakul P, Yachantha C, et al. Renal tubular cell damage and oxidative stress in renal stone patients and the effect of potassium citrate treatment. *Urol Res.* 2005; 33:65–69. [PubMed: 15565439]
9. Thamilselvan S, Hackett RL, Khan SR. Lipid peroxidation in ethylene glycol induced hyperoxaluria and calcium oxalate nephrolithiasis. *J Urol.* 1997; 157:1059–1063. [PubMed: 9072543]
10. Denhardt DT, Noda M, O'Regan AW, et al. Osteopontin as a means to cope with environmental insults: regulation of inflammation, tissue remodeling, and cell survival. *J Clin Invest.* 2001; 107:1055–1061. [PubMed: 11342566]
11. Persy VP, Verstrepen WA, Ysebaert DK, et al. Differences in osteopontin up-regulation between proximal and distal tubules after renal ischemia/reperfusion. *Kidney Int.* 1999; 56:601–611. [PubMed: 10432399]
12. Xie Y, Sakatsume M, Nishi S, et al. Expression, roles, receptors, and regulation of osteopontin in the kidney. *Kidney Int.* 2001; 60:1645–1657. [PubMed: 11703581]

13. Khan SR, Johnson JM, Peck AB, et al. Expression of osteopontin in rat kidneys: induction during ethylene glycol induced calcium oxalate nephrolithiasis. *J Urol.* 2002; 168:1173–1181. [PubMed: 12187263]
14. Verhulst A, Asselman M, Persy VP, et al. Crystal retention capacity of cells in the human nephron: involvement of CD44 and its ligands hyaluronic acid and osteopontin in the transition of a crystal binding- into a nonadherent epithelium. *J Am Soc Nephrol.* 2003; 14:107–115. [PubMed: 12506143]
15. Verkoelen CF, Verhulst A. Proposed mechanisms in renal tubular crystal retention. *Kidney Int.* 2007; 72:13–18. [PubMed: 17429341]
16. Asselman M, Verhulst A, Van Ballegooijen ES, et al. Hyaluronan is apically secreted and expressed by proliferating or regenerating renal tubular cells. *Kidney Int.* 2005; 68:71–83. [PubMed: 15954897]
17. Verhulst A, Asselman M, De Naeyer S, et al. Preconditioning of the distal tubular epithelium of the human kidney precedes nephrocalcinosis. *Kidney Int.* 2005; 68:1643–1647. [PubMed: 16164641]
18. Khan SR, Glenton PA. Deposition of calcium phosphate and calcium oxalate crystals in the kidneys. *J Urol.* 1995; 153:811–817. [PubMed: 7861545]
19. Atmani F, Slimani Y, Mimouni M, et al. Effect of aqueous extract from *Herniaria hirsuta* L. on experimentally nephrolithiasic rats. *J Ethnopharmacol.* 2004; 95:87–93. [PubMed: 15374612]
20. Khan SR. Animal models of kidney stone formation: an analysis. *World J Urol.* 1997; 15:236–243. [PubMed: 9280052]
21. Fan J, Glass M, Chandhoke P. Impact of ammonium chloride administration on a rat ethylene glycol urolithiasis model. *Scanning Microsc.* 1999; 13:299–306.
22. Huang HS, Chen J, Chen CF, et al. Vitamin E attenuates crystal formation in rat kidneys: roles of renal tubular cell death and crystallization inhibitors. *Kidney Int.* 2006; 70:699–710. [PubMed: 16807540]
23. Huang HS, Chen CF, Chien CT, et al. Possible biphasic changes of free radicals in ethylene glycol-induced nephrolithiasis in rats. *BJU Int.* 2000; 85:1143–1149. [PubMed: 10848711]
24. Huang HS, Ma MC, Chen J, et al. Changes in the oxidant-antioxidant balance in the kidney of rats with nephrolithiasis induced by ethylene glycol. *J Urol.* 2002; 167:2584–2593. [PubMed: 11992092]
25. Sumathi R, Jayanthi S, Kalpanadevi V, et al. Effect of DL alpha-lipoic acid on tissue lipid peroxidation and antioxidant systems in normal and glycollate treated rats. *Pharmacol Res.* 1993; 27:309–318. [PubMed: 8367380]
26. Packer L, Weber SU, Rimbach G. Molecular aspects of alpha-tocotrienol antioxidant action and cell signalling. *J Nutr.* 2001; 131:369S–373S. [PubMed: 11160563]
27. Tsujihata M. Mechanism of calcium oxalate renal stone formation and renal tubular cell injury. *Int J Urol.* 2008; 15:115–120. [PubMed: 18269444]
28. Thamilselvan S, Khan SR, Menon M. Oxalate and calcium oxalate mediated free radical toxicity in renal epithelial cells: effect of antioxidants. *Urol Res.* 2003; 31:3–9. [PubMed: 12624656]
29. Thamilselvan S, Menon M. Vitamin E therapy prevents hyperoxaluria-induced calcium oxalate crystal deposition in the kidney by improving renal tissue antioxidant status. *BJU Int.* 2005; 96:117–126. [PubMed: 15963133]
30. Schepers MS, van Ballegooijen ES, Bangma CH, et al. Crystals cause acute necrotic cell death in renal proximal tubule cells, but not in collecting tubule cells. *Kidney Int.* 2005; 68:1543–1553. [PubMed: 16164631]
31. Green ML, Freel RW, Hatch M. Lipid peroxidation is not the underlying cause of renal injury in hyperoxaluric rats. *Kidney Int.* 2005; 68:2629–2638. [PubMed: 16316339]
32. Khan SR. Hyperoxaluria-induced oxidative stress and antioxidants for renal protection. *Urol Res.* 2005; 33:349–357. [PubMed: 16292585]
33. Zecher M, Guichard C, Velasquez MJ, et al. Implications of oxidative stress in the pathophysiology of obstructive uropathy. *Urol Res.* 2009; 37:19–26. [PubMed: 19082822]
34. Grasl-Kraupp B, Ruttka-Nedecky B, Koudelka H, et al. In situ detection of fragmented DNA (TUNEL assay) fails to discriminate among apoptosis, necrosis, and autolytic cell death: a cautionary note. *Hepatology.* 1995; 21:1465–1468. [PubMed: 7737654]

35. Huh JE, Lee EO, Kim MS, et al. Penta-O-galloyl-beta-D-glucose suppresses tumor growth via inhibition of angiogenesis and stimulation of apoptosis: roles of cyclooxygenase-2 and mitogen-activated protein kinase pathways. *Carcinogenesis*. 2005; 26:1436–1445. [PubMed: 15845650]
36. Tiselius HG, Ferraz RR, Heilberg IP. An approximate estimate of the ion-activity product of calcium oxalate in rat urine. *Urol Res*. 2003; 31:410–413. [PubMed: 14579106]
37. Dorrenhaus A, Muller JI, Golka K, et al. Cultures of exfoliated epithelial cells from different locations of the human urinary tract and the renal tubular system. *Arch Toxicol*. 2000; 74:618–626. [PubMed: 11201669]
38. Greene EL, Farrell G, Yu S, et al. Renal cell adaptation to oxalate. *Urol Res*. 2005; 33:340–348. [PubMed: 16284879]

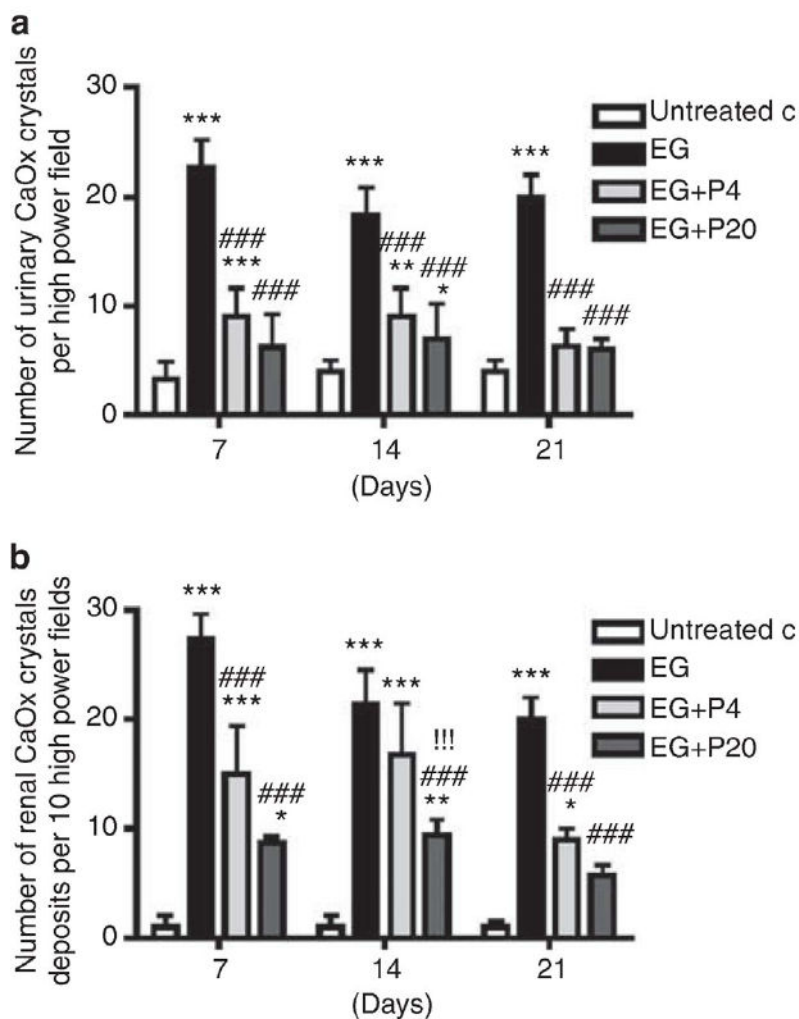


Figure 1. Effect of 1,2,3,4,6-penta-O-galloyl-b-D-glucose (PGG) on calcium oxalate (CaOx) crystal deposition in ethylene glycol (EG)-treated rat urine and kidneys

(a) Twenty-four hour rat urine samples on days 7, 14, and 21 were collected on ice in a metabolic cage and CaOx crystals with tetragonal bipyramidal habit were counted in a hemocytometer at X400 magnification. Graph represents the average number of urinary CaOx crystals in the rat urine per high power field. (b) Histological specimens of rat kidney tissues (n=6/group) obtained on days 7, 14, and 21 following EG treatment were stained with hematoxylin and eosin (H&E), and the number of crystal depositions was counted. Graph represents the average number of crystal depositions in the kidney per high power field. Data represent means \pm s.d. *P<0.05, **P<0.01, and ***P<0.001 versus untreated control; ###P<0.001 versus EG; and !!!P<0.001 versus EG+P4 two-way analysis of variance followed by a post hoc analysis. C, untreated control (distilled water); EG, EG-treated group (0.8% EG/1% ammonium chloride (AC) (NH₄Cl) in drinking water); and EG+P4 and EG+P20, two EG- and PGG-treated groups (0.8% EG/1% AC + 4 or 20 mg/kg of PGG in 2% methylcellulose).

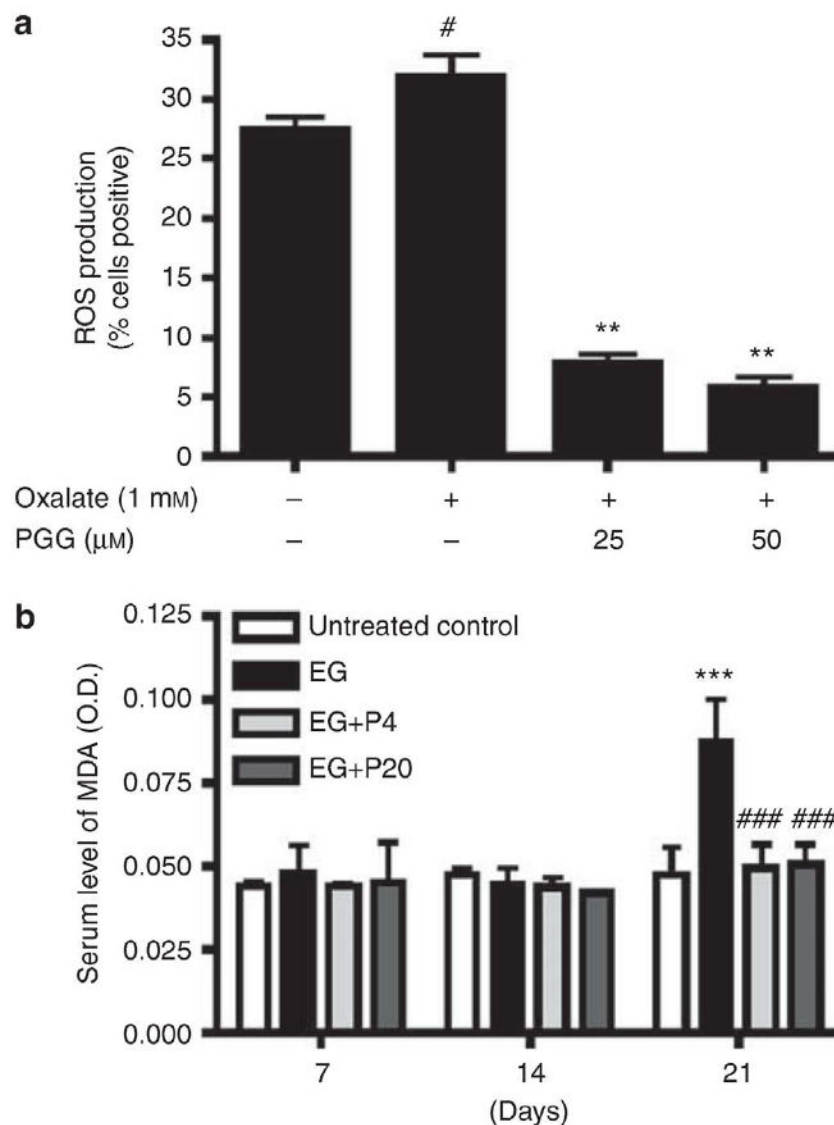


Figure 2. Effect of 1,2,3,4,6-penta-O-galloyl-b-D-glucose (PGG) on ROS production in human renal cells (HRCs) exposed to calcium oxalate (1mM) and on the serum malondialdehyde (MDA) level in ethylene glycol (EG)-treated rats

(a) The levels of ROS in HRCs were measured using ROS-sensitive fluorometric probe, 2,7-dichlorofluorescein by flow cytometric analysis. Data are expressed as % cells positive.

Data represent means \pm s.d. #P<0.05 versus untreated control and **P<0.01 versus oxalate.

(b) The level of serum MDA was determined on days 7, 14, and 21 following EG treatment (n=6/group) by enzyme-linked immunosorbent assay colorimetric method. Data represent means \pm s.d. ***P<0.001 versus untreated control and ###P<0.001 versus EG, two-way

analysis of variance followed by a post hoc analysis. C, untreated control (distilled water); EG, EG-treated group (0.8% EG/1% ammonium chloride (AC; NH₄Cl) in drinking water); and EGpP4 and EGpP20, two PGG-treated groups (0.8% EG/1% ACp4 or 20 mg/kg of PGG in 2% methylcellulose).

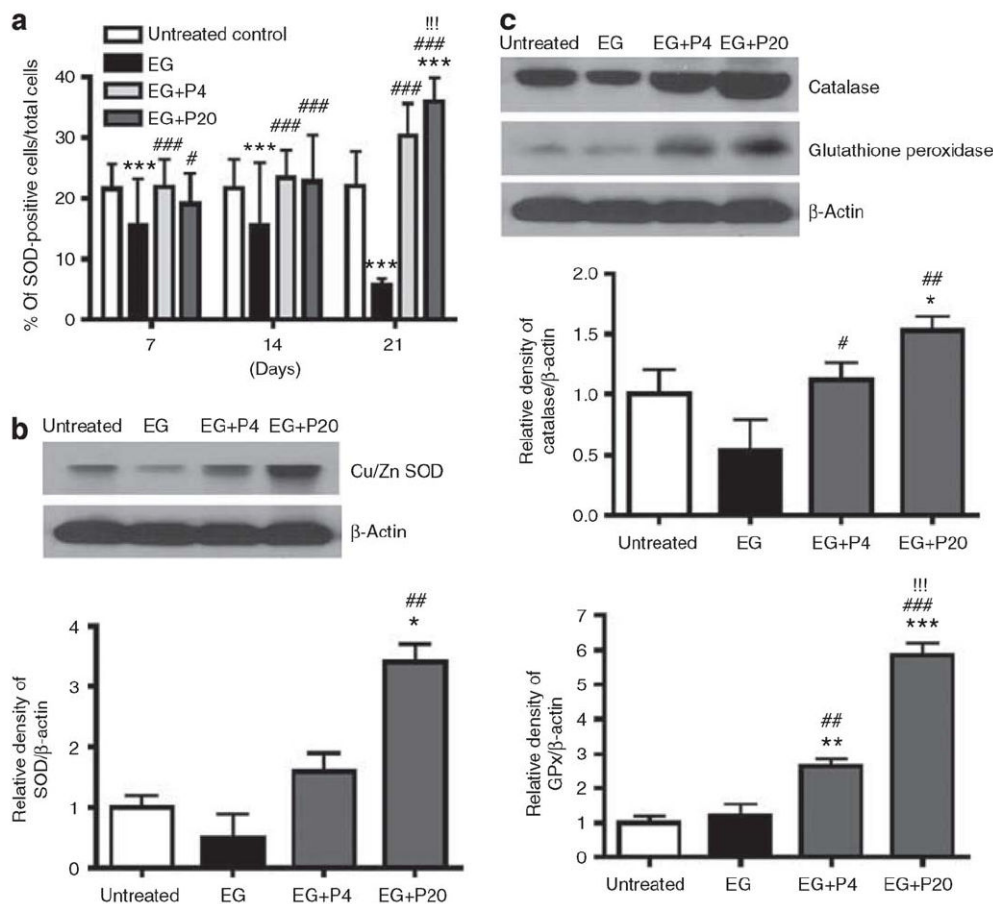


Figure 3. Effect of 1,2,3,4,6-penta-O-galloyl-b-D-glucose (PGG) on antioxidant enzyme activity in ethylene glycol (EG)-treated rat kidneys

(a) Immunohistochemical staining for superoxide dismutase (SOD) expression in rat kidney tissues ($n=46$ /group) obtained on days 7, 14, and 21 following EG treatment was performed and the average number of positive stained cells per high power field was counted from three independent experiments. Data represent means \pm s.d. *** P <0.001 versus untreated control; # P <0.05 and ### P <0.001 versus EG; and !!! P <0.001 versus EG+P4, two-way analysis of variance followed by a post hoc analysis. (b–c) Western blot analysis in EG-treated rat kidneys on day 21 following EG treatment for Cu/Zn SOD (b), catalase (c), glutathione peroxidase (c), and b-actin. Data of protein expression represent means \pm s.d. * P <0.05 versus untreated control and ## P <0.01 versus EG, one-way analysis of variance followed by a post hoc analysis. C, untreated control (distilled water); EG, EG-treated group (0.8% EG/1% ammonium chloride (AC; NH_4Cl) in drinking water); and EG+P4 and EG+P20, two PGG-treated groups (0.8% EG/1% AC+4 or 20 mg/kg of PGG in 2% methylcellulose).

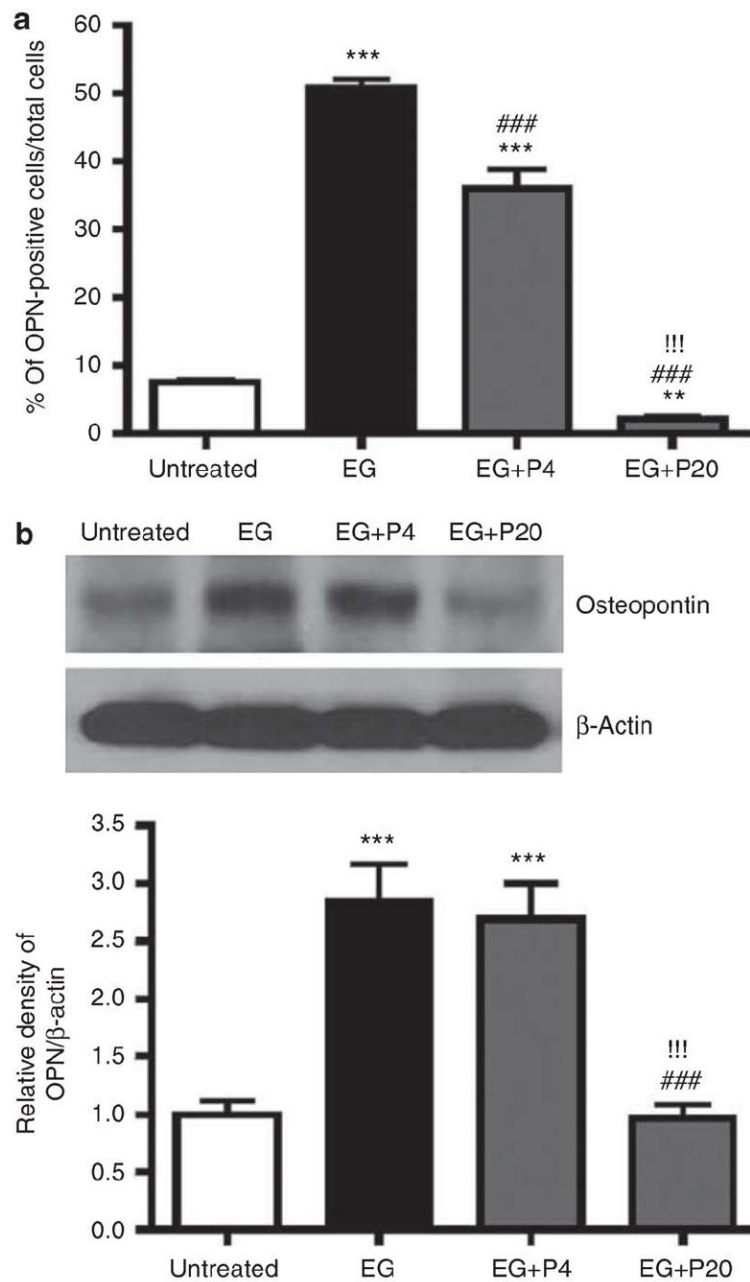


Figure 4. Effect of 1,2,3,4,6-penta-O-galloyl-b-D-glucose (PGG) on osteopontin (OPN) expression in ethylene glycol (EG)-treated rat kidneys

(a) Immunohistochemical staining for OPN in rat kidney tissues (n¹/46/group) obtained on day 21 following EG treatment was performed and the average number of stained cells per high power field was counted from three independent experiments. Data represent means \pm s.d. (b) Western blot analysis in EG-treated rat kidneys for OPN and b-actin. ***P<0.001 versus untreated control; ###P<0.001 versus EG; and !!!P<0.001 versus EG+P4, one-way analysis of variance followed by a post hoc analysis. C, untreated control (distilled water); EG, EG-treated group (0.8% EG/1% ammonium chloride (AC; NH₄Cl) in drinking water);

and EG+P4 and EG+P20, two PGG-treated groups (0.8% EG/1% ACp4 or 20 mg/kg of PGG in 2% methylcellulose).

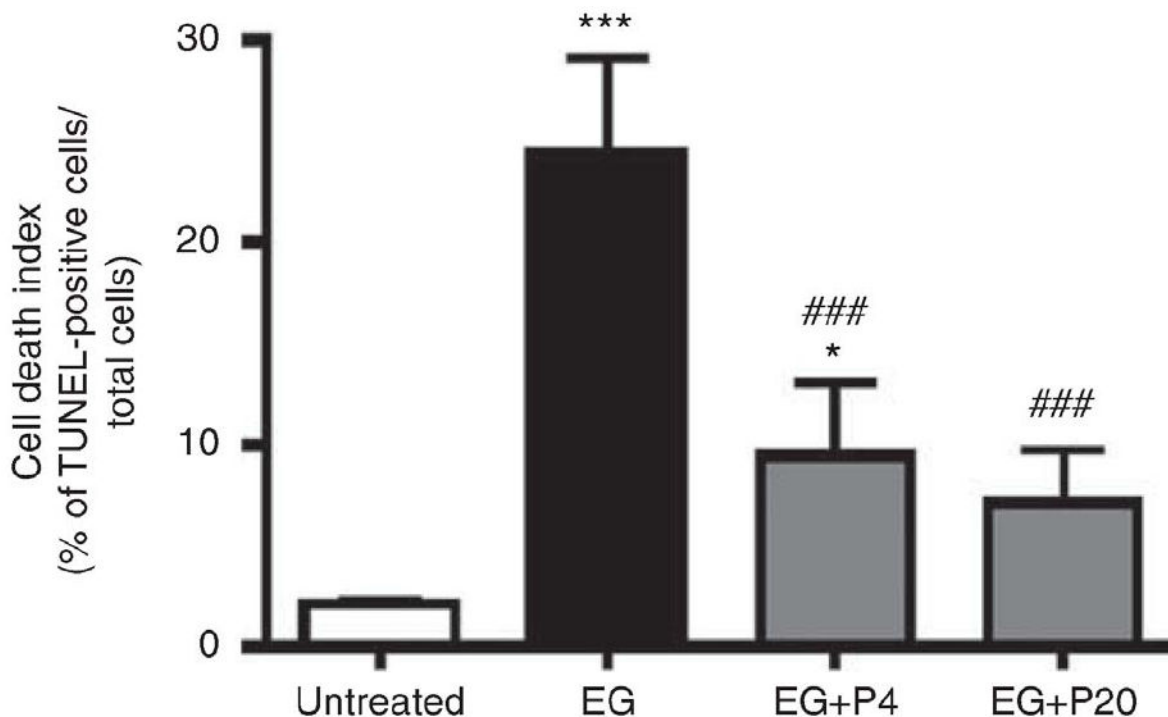


Figure 5. Effect of PGG on cell death index TUNEL staining in EG treated rat kidneys
 Cell death was assessed by TUNEL assay in rat kidney tissues (n¹/₄6/group) obtained on day 21 following EG treatment. Graph represents the average number of TUNEL positive stained cells per high power field. Data represent means±s.d. ###P<0.001 versus untreated control, and *P<0.05 and ***P<0.001 versus untreated control, ###P<0.001 versus EG, two-way analysis of variance followed by a post hoc analysis. C, untreated control (distilled water); EG, EG treated group (0.8% EG/1% AC (NH₄Cl) in drinking water) and, EG+P4 and EG+P20; two PGG-treated groups (0.8% EG/1% AC+4 or 20mg/kg of PGG in 2% methylcellulose).

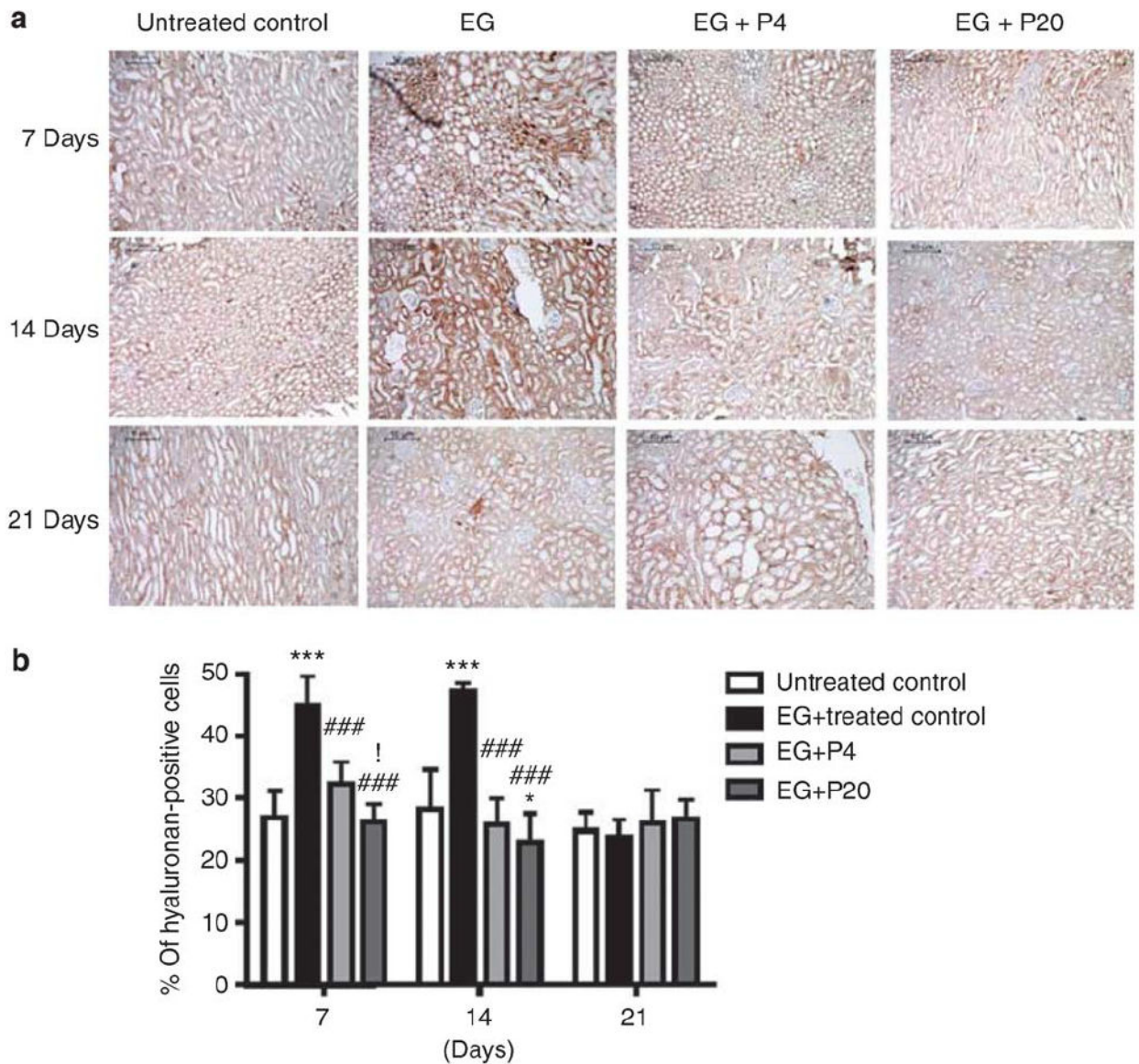


Figure 6. Effect of 1,2,3,4,6-penta-O-galloyl-b-D-glucose (PGG) on hyaluronan expression in ethylene glycol (EG)-treated rat kidneys
 (a) Immunohistochemical staining for renal hyaluronan expression in EG-treated rat kidneys (n=46/group) obtained on days 7, 14, and 21 following EG treatment. (b) The average number of hyaluronan-positive stained cells per high power field. Data represent means±s.d. *P<0.05 and ***P<0.001 versus untreated control; ###P<0.001 versus EG; and !P<0.05 versus EG+P4, two-way analysis of variance followed by a post hoc analysis. C, untreated control (distilled water); EG, EG-treated group (0.8% EG/1% ammonium chloride (AC; NH₄Cl) in drinking water); and EG+P4 and EG+P20, two PGG-treated groups (0.8% EG/1% AC+P4 or 20 mg/kg of PGG in 2% methylcellulose).

Table 1

Urine Chemistry

Group	Days after EG Treatment	Volume (ml)	pH	Calcium (mg/day)	Oxalate (mg/day)	AP (CaOx) index
Untreated Control	7 (n=6)	12.66±2.510	7.33±0.577	5.33±1.250	7.21±1.003	2.265±0.136
	14 (n=6)	14.30±1.154	8.00±0.001	5.25±0.350	6.93±1.000	2.179±0.033
	21 (n=6)	25.00±5.000	7.33±0.577	3.53±0.250	6.82±1.007	2.144±0.029
EGT-Treated control	7 (n=6)	14.33±5.130	6.33±0.577	2.96±1.360	11.97±1.000	3.761±0.282*
	14 (n=4)	18.33±2.880	6.75±0.957	6.50±2.680	12.30±1.026	3.876±1.036*
	21 (n=6)	18.80±4.810	6.00±0.001*	4.86±1.270	12.50±1.018*	3.933±1.506**
EG+PPG (4 mg/kg)	7 (n=6)	18.60±4.040	6.33±0.577	3.90±1.120	10.56±1.010	3.319±0.496
	14 (n=5)	17.50±5.060	6.00±0.001	3.50±1.760##	9.56±1.030*	2.787±0.712
	21 (n=6)	30.00±7.900	6.60±1.341	1.70±0.200##	9.86±1.000#	3.098±0.354
EG+PPG (20 mg/kg)	7 (n=6)	15.33±4.610	7.16±0.288	2.80±1.550	8.13±1.006	2.552±0.261##
	14 (n=6)	17.60±7.820	6.20±0.447	3.10±1.650##	8.87±1.017	2.564±0.099#
	21 (n=5)	31.50±12.700	6.00±0.001	1.73±0.005##	9.49±1.0130##	2.928±0.547

Abbreviations: CaOx, calcium oxalate; EG, ethylene glycol; PGG, 1,2,3,4,6-penta-O-galloyl-b-D-glucose. Urinary oxalate excretion was measured by an enzymatic method using oxalate oxidase. Urinary calcium excretion was measured using Hitachi 747 automatic analyzer by ion selective electrode method. AP index was calculated with the urinary values of oxalate, calcium, magnesium, citrate, and volume, according to AP index formula: $[(4067 \times \text{Ca}^{0.93} \times \text{Ox}^{0.96}) \times (\text{Mg}^{0.55} \times (\text{Cit}+0.015)^{0.60} \times \text{V}^{0.99})]$. Data represent means±s.d.

* P<0.05 and

** P<0.01 versus untreated control;

P<0.05 and

P<0.01 versus EG, two-way analysis of variance followed by post hoc analysis.

Table 2

Blood Chemistry

Group	Days after EG Treatment	Albumin (g/dl)	Creatinine (mg/dl)	BUN (mg/dl)
Untreated Control	7 (n=6)	4.2±0.305	0.6±0.577	18.3±2.870
	14 (n=6)	4.5±0.556	0.8±0.115	20.6±2.084
	21 (n=6)	4.6±0.519	0.7±0.100	18.1±0.500
EG-Treated control	7 (n=6)	3.8±0.070	0.6±0.070	16.9±3.110
	14 (n=4)	3.5±0.173**	0.6±0.141	24.6±15.90
	21 (n=6)	3.8±0.273*	0.6±0.044	14.5±1.134
EG+PGG (4 mg/kg)	7 (n=6)	3.9±0.305	0.5±0.057	17.6±4.650
	14 (n=5)	3.8±0.298	0.6±0.050	19.2±4.860
	21 (n=6)	4.1±0.597	0.6±0.173	19.2±7.947
EG+PGG (20 mg/kg)	7 (n=6)	4.0±0.353	0.6±0.141	19.5±2.330
	14 (n=6)	3.7±0.125*	0.6±0.057	15.2±2.610
	21 (n=5)	4.2±0.714	0.7±0.057	14.0±1.997

Abbreviations: BUN, blood urea nitrogen; EG, ethylene glycol; PGG, 1,2,3,4,6-penta-O-galloyl- β -D-glucose.

Mean±s.d.

* P<0.05 and

** P<0.01 versus untreated control, two-way analysis of variance followed by post hoc analysis.